CUK CONVERTER BASED LLC RESONANCE FOR DC-DC BOOSTING APPLICATIONS

S.Sanny Kumar[1], N. Prasanth Babu[2]

[1]M.Tech Scholar (PS), [2] Asst. Professor Deptt of EEE

Nalanda Institute of Engg and Tech. (NIET), Siddharth Nagar, Guntur, A.P. (India)

ABSTRACT

*Here**, in this paper, resonant tank model system and practical method considerations are exited for a high production LLC multi resonant dc–dc conversion in a two-ways efficient battery charger for district electric vehicle implementation. The multi resonant controlling has been analysed and its production characteristics are occurred. It removes both low- and high frequency current ripple quantity on the battery system this maximizing battery life time without punishes the magnitude of the charger. Simulation and fact-finding results are proposed for a prototype module unit conversion of 390V come from the input dc link to an output system voltage range of 48–72V dc at 650 W. The basically prototype improves a system of peak efficiency is maximum of 96%.*

Keyword: Battery Supplies, Dc–Dc Power Conversion Devices, an Electrical Operating Vehicle, a Resonant Operating Converter

I. INTRODUCTION

Neighbourhood of an electrical operating vehicle (NEVs) are prompt by an electric motor this is applied with power from a rechargeable battery system source. Basically, the production characteristics generated for many electrical vehicles (EV) approaches far more the storage unit this improves of conventional method of battery systems. However, battery methodology is increasing and as this transition appears the charging of these batteries units having very difficulties due to the high voltages and currents included in the system and an experienced charging of algorithms methods. easterly charging of more capacity battery packages effects maximum increased unwanted disturbances in the ac advantage to power system, here by increasing the used for more efficient, less-distortion of smart chargers. A modish charger is a battery charger this could response to the conditions of a battery and rectifies its charging movements according to the battery system algorithms. Meanwhile, a standard, or basic battery charger provide a constant magnitude of dc or pulsed magnitude of dc power supply to a battery having charged The desired NEV battery charger system of power module involves an ac–dc conversion with power factor correction process followed by a remote dc–dc converter system, as appears in Fig. 1.
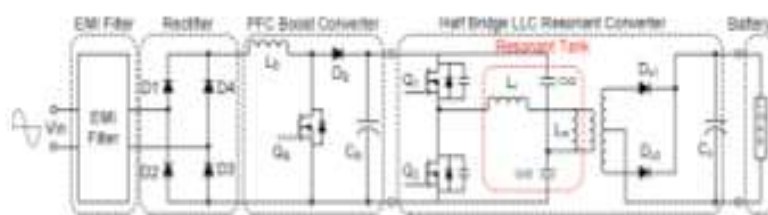

Fig. 1 Typical Battery Charging Power Architecture

This model architecture of effectively removes the low- and high-frequency order current ripples charging in the battery unit without using a higher filter capacitor method of an alternative it is worn a high-frequency transformer connection. The model of architecture increases the battery life cycle without corrects the chargers volume model. In this work results, the front-end uses ac–dc PFC converter. it is a conventional method of continuous conduction mode boost technique and the second-stage is dc–dc converter is a half-bridge has many resonant LLC converter. The selection for choosing the type of methods that include high reliability system, high efficiency operation and low component of cost. The half-bridge a resonant LLC converter is mainly used in the telecom industry for its higher efficiency at the resonant frequency occur and its capability to control the output voltage throughout the hold-up time period, while the output voltage is a constant and the input voltage might be dropped outstandingly.
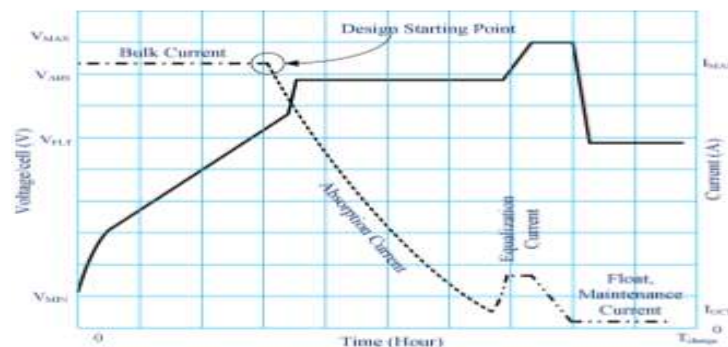

Fig. 2 Simplified Adaptive 4-Step Lead Acid Battery Charging Profile

This battery voltage source at the dc–dc converter output could be vary from as low as 36 V to as high as 72 V. Therefore, the Model design requirements for choosing the resonant tank parameter components are importantly different than those in telecom application purpose promote a constant output voltage source.

II. DESIGN PROCEDURE

The life time and capacity of EV batteries based on many factors, like as cycle counter, charge mode method, maintenance of system, temperature and age. More these reasons, the charge mode have a important impact on battery life time and the range of capacity. EV batteries could be charge with current and voltage magnitude levels with low ripple quality.

To decrease the switching losses than result from high-frequency process, resonant power transformation can be used. There are more publications and applications are noted in industrial More on resonant circuit design process. There are two main issues with the present work: 1) the output voltage is taking constant which is not a correct consideration in battery charging and 2) the ratio of the transformer of magnetizing inductance and the resonant inductance is taken by some considerable values without taking into considering the result of the short circuit conditions on the resonant network.

2.1 INITIAL DESIGN PARAMETERS

The input voltage scope, output voltage span, maximum output power and resonant frequency are the initial model design parameters to be explained. The input voltage to the dc–dc phase is resolved by the PFC bus output voltage at the dc link capacitors. Dissimilar telecom power supply applications, those are no hold-up time demand and the variation seen by the LLC converter has only the low-frequency ripple content on the PFC bus capacitors.

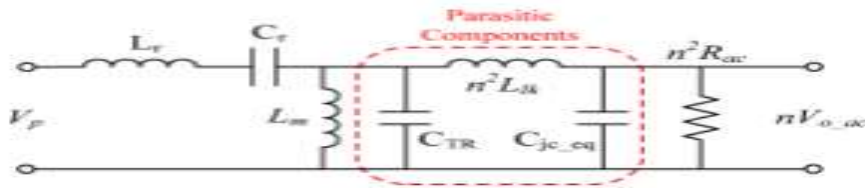## 2.2 Maximum Switching Frequency, Maximum Dead Time

Fig. 3 AC Equivalent Circuit of LLC Resonant Converter Including Parasitic Components

The ac equivalent circuit of an LLC resonant converter adding parasitic components. The normal dc gain equation as the converter is changed by the addition of the rectifier diode link capacitances and as a effect improved the switching frequency reduced the output voltage till, the circuit resonates with the diode junction capacitances at while point, moreover increasing the switching frequency it results to increase the range of output voltage.

2.3 Selecting Transformer Turns Ratio, Nn

The transformer turns factor ratio could be selected at the resonant frequency while the gain is constant and could be measured using (1), where Vd represents the diode voltage drop of the output rectifier

$$N_n = \frac{V_{\text{in(nom)}}}{2(V_{o(\text{min})} + V_d)}. \tag{1}$$

2.4 Calculating Resonant Inductor, Lr

The minimum resonant inductor might be chosen to limit range of maximum output current in the short circuit state and limit range of converter to its peak switching frequency. The minimum value of inductance is given by (2)

$$L_{r(\text{SCC})} = \frac{N_n \cdot V_{\text{in(nom)}} \cdot V_{o(\text{nom})}}{8 f_{s\_\text{max}} \cdot P_o}. \tag{2}$$

2.5 Calculating Resonant Capacitor, Cr

Once the range of value of the resonant inductor is resolute, the resonant capacitor value have be measured using (3)

$$C_{r(\text{res})} = \frac{1}{(2 \cdot \pi \cdot f_o)^2 \cdot L_{r(\text{scc})}}. \tag{3}$$

2.6 Characteristic Impedance and Quality Factor

After calculating the value of resonant inductor and capacitor value, the characteristic impedance of the resonant network is taken by (4)

$$Z_o = \sqrt{\frac{L_{r(\text{scc})}}{C_{r(\text{res})}}}. \tag{4}$$

The minimum quality factor can then be determined by using (5) and (6) as shown.

$$Q_{\min} = \frac{Z_o}{R_{\text{ac\_max}}} \tag{5}$$

$$R_{\text{ac\_max}} = \frac{8N_n^2}{\pi^2} \frac{V_{o\_\text{max}}^2}{P_o}. \tag{6}$$

2.7 Calculating Magnetizing Inductance, Lm

The option of magnetizing inductance has to full fill two states. First, to attain ZVS below no load conditions, a peak magnetizing inductance, Lm(ZVS),is taken as given by (7). In (7), the total capacitance of the half-bridge, there are Q1 and Q2 MOSFET output values of capacitances and the transformer and included inductor internal-winding capacitances. In order to achieve the need maximum gain at the minimum switching frequency as in [27], Lm(max) is given by (8)

$$L_{m(ZVS)} = \frac{t_{\text{dead}} \cdot N_n \cdot V_{o(\min)} \cdot \left(\frac{1}{4 \cdot f_{s\_max}} - \frac{t_{\text{dead}}}{2} \right)}{C_{\text{HB}} \cdot V_{\text{in}(\max)}} \qquad (7)$$

$$L_{m(\max)} = L_{r(\text{sec})} \frac{\pi^2}{4} \frac{\frac{f_o}{f_{s\_min}} - 1}{1 - \frac{1}{M_{dc\_max}}}. \qquad (8)$$

The final limit of value used for the magnetizing inductance is the minimum of the two values. Though, if Lm(max) <Lm(ZVS),then a new peak time could be measured using the value from Lm(max), and replaced in (7) to get a new value of dead time. Finally, the total inductance value range must content the energy balance in the total capacitance of the half-bridge, using equations (9) and (10)

$$\frac{1}{2}(L_{m(\min)} + L_{r(\text{sec})})I_{m\_pk}^2 > \frac{1}{2}C_{\text{HB}}V_{\text{in}(\max)}^2 \qquad (9)$$

$$I_{m\_pk} = \frac{N_n V_{o(\min)} T_o}{4L_m}. \qquad (10)$$

III. PRACTICAL DESIGN CONSIDERATIONS

A complete model of design procedure and the range of resonant tank component method are provided in the above section. Additional the practical model of design considerations are addressing MOSFET method of selection resonant and the range of output capacitor selection and output diode rectifier selection, controller IC selection. The power and current limit limitations are provided in the sub-sections that follow as.

3.1 MOSFET Selection

For MOSFET choice, consideration can be given to practical method dv/dt turn-on limits, but diode reverse retrieval and losses. Fig.6 shows the voltage beyond the resonant capacitor and the value of current flow through the MOSFET as a function of time at turn-on, while the switching frequency is below the unity gain resonant frequency.

$$\theta = \text{Arcsin}\left(\frac{N_n V_o T_o}{4L_m I_{\text{PK}}} \right). \qquad (12)$$

The switch RMS current can be calculate during (13)

$$I_{\text{MOSFET\_rms}} = \sqrt{\frac{2}{T_s} \int_0^{\frac{T_s}{2}} (I_{\text{MOSFET}}(t))^2 \, dt}. \qquad (13)$$

The MOSFET RMS current as a part of output voltage at minimum level, nominal and the range of maximum input voltages (PFC bus voltage). It is used that this design model is only used for switching frequencies under the constant gain resonant frequency.

The drain to source (CDS) and gate to source (CGS) process the intrinsic capacitors. While the drain voltage maximum reaches to approximately10V, then across it starts to reduced suddenly up to 100 times at 40 V and

then drain current has to continuously to flowing through the CDS and the MOSFET channel. If the MOSFET channel current is zero, than the results in lossless will be switch-off.

3.2 Resonant and Output Capacitor Selection

The value of resonant range of capacitor voltage is approximately associated with the resonant inductor current, while as partially the same like as the MOSFET current. By the definition, the voltage across the resonant capacitor is given by (14), By the allowing the capacitor peak-to-peak voltage to be expressed as (15)

$$V_{C_{pk-pk}} = \frac{\text{Total Charge}}{C_{r(res)}} \qquad (14)$$

$$V_{C_{pk-pk}} = \frac{\int_0^{\frac{T_s}{2}} |I_{MOSFET}(t)|\, dt}{C_{r(res)}}. \qquad (15)$$

Let, assuming the voltage waveform is sinusoidal process the average dc and RMS ac values of the resonant capacitor are ta by (16) and (17), respectively

$$V_{C_{dc}} = \frac{V_{in}}{2} \qquad (16)$$

$$V_{C_{ac\_rms}} = \frac{V_{C_{pk-pk}}}{2\sqrt{2}}. \qquad (17)$$

In order to exhibit the output capacitor ac ripple current then secondary side as instantaneous current is need and is given by (18), enabling the output capacitor ac ripple current to be measured using (19)–(21)

$$I_{o\_sec}(t) = N_n I_{MOSFET}(t) + N_n^2 \frac{V_o T_o}{4L_m}\left(\frac{T_o}{4} - 1\right) \qquad (18)$$

$$I_{o\_sec\_ac} = \sqrt{I_{o\_sec\_rms}^2 - I_{o\_sec\_ave}^2} \qquad (19)$$

$$I_{o\_sec\_rms} = \sqrt{\frac{1}{T_o}\int_0^{\frac{T_o}{2}} I_{o\_sec}(t)^2\, dt} \qquad (20)$$

$$I_{o\_sec\_ave} = \frac{1}{T_o}\int_0^{\frac{T_o}{2}} I_{o\_sec}(t)\, dt. \qquad (21)$$

The output value of capacitor ac ripple current as a purpose of output voltage for different input voltages. As can be taken, the a cripple current is a tit speak, when the both input voltage and output voltage. For this purpose the metalize polyester bank capacitors are best suited.

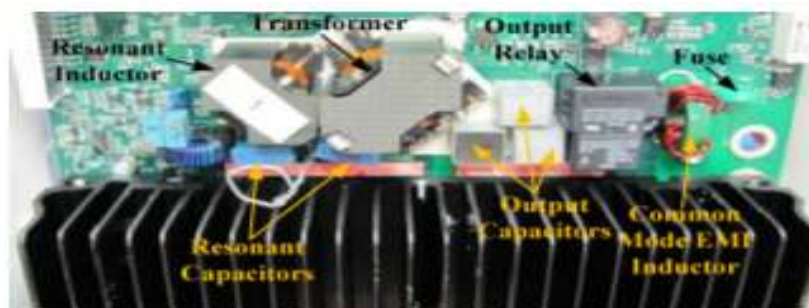### 3.3 Output Diode Rectifier Selection

Fig.4. Photo of the Prototype LLC Dc–Dc Converter

The output when diode rectifiers performs ZCS for both turn-on (zero di/dt) and turn-off. So, the parameter values to taking in the selection process of the diodes are forward dropped. The VFWD and range of junction capacitance, Cj. The available uses of technologies included Schottky and ultrafast diodes.

3.4 Power Limit and Current Limit Restrictions

The values of output current and output voltage are controlled by the feedback control circuit process as per the voltage and current references provided by the battery charging algorithm requirements. Then, the output power range at ion has two distinct curves. The actual power limit is implemented by software, as a hyperbolic function given by (22)

$$I_o = \frac{P_o(\text{Const.})}{V_o}. \qquad (22)$$

3.5 Control IC Selection

There are many commercial off-the-shelf control methods ICs availability for LLC resonant converters while each having distinct characteristics and limitations. The maim key requirements for selecting an controller are the switching frequency range method, operating temperature range, ability to control the secondary side, the programmable dead time, the programmable soft start, the protection and brownout detection.

IV. EXPERIMENTAL RESULTS

A prototype model of the half-bridge LLC multi resonant converter was builted to produce a proof-of-concept and modify the analytical manner of work presented. Then these measurements values were considered with the output relay process the common mode EMI inductor and output fuse added. So, the Experimental results of waveforms of the resonant tank current, resonant capability or voltage and voltage across bottom MOSFET,Q2 are provided.

V. CONCLUSION

A resonant tank model design process and practical design considerations were donate for a high performance an LLC multi resonant dc–dc converter in a two methods large output voltage range dapper battery charger for NEV operation. This multi resonant converter have been analysed and its operating characteristics values presented. It avoids both the low- and high-frequency current ripples on the battery, this maximizing battery life without correct the volume of this charger.

REFERENCES

[1]   D.W. Gao, C. Mi, and A. Emadi, "Modeling and simulation of electric and hybrid vehicles," Proc. IEEE, vol. 95, no. 4, pp. 729–745, Apr. 2007.

[2]   A. Emadi, S. Williamson, and A. Khaligh, "Power electronics intensive solutions for advanced electric, hybrid electric, and fuel cell vehicular power systems," IEEE Trans. Power Electron., vol. 21, no. 3, pp. 567– 577, May 2006.

[3]   A. M. Rahimi, "A lithium-ion battery charger for charging up to eight cells,"inProc.IEEEConf.VehiclePowerPropulsion, 2005, pp.131–136.

[4]   B. Singh, B. N. Singh, A. Chandra, K. Al-Haddad, A. Pandey, and D. P. Kothari, "A review of single-phase improved power quality ACDC converters," IEEE Trans. Ind. Electron., vol. 50, no. 5, pp. 962–981, Oct. 2003.

[5]   L. Petersen and M. Andersen, "Two-stage power factor corrected power supplies: The low component-stress approach, "in Proc. IEEE Appl. Power Electron. Conf. Expo., 2002, vol. 2, pp. 1195–1201.

[6]   B. Lu, W. Dong, S. Wang, and F. C. Lee, "High frequency investigation of single-switch CCM power factor correction converter," in Proc. IEEE Appl. Power Electron. Conf. Expo., 2004, vol. 3, pp. 1481–1487.

[7]   L. Yang, B. Lu, W. Dong, Z. Lu, M. Xu, F. C. Lee, and W. G. Odendaal, "Modeling and characterization of a 1KW CCM PFC converter for conducted EMI prediction, "in Proc. IEEE Appl. Power Electron. Conf. Expo., 2004, vol. 2, pp. 763–769.

[8]   A. K. S. Bhat, "Analysis and design of LCL-type series resonant converter," IEEE Trans. Ind. Electron., vol. 41, no. 1, pp. 118–124, Feb. 1994.

[9]   B. Yang, F. C. Lee, A. J. Zhang, and G. Huang, "LLC resonant converter for front end DC/DC conversion," in Proc. IEEE Appl. Power Electron. Conf. Expo., 2002, vol. 2, pp. 1108–1112.

[10] T. Liu, Z. Zhou, A. Xiong, J. Zeng, and J. Ying, "A novel precise design method for LLC series resonant converter," in Proc. IEEE Telecommun. Energy Conf., INTELEC, 2006, pp. 1–6.

[11] Jee-hoon Jung and Joong-gi Kwon, "Theoretical analysis and optimal design of LLC resonant converter," in Proc. Eur. Conf. Power Electron. Appl., 2007, pp. 1–10.

[12] J.Biela,U.Badstubneran J. W.Kolar,"Designofa5kW,1U,10kW/ltr resonant DC-DC converter for telecom applications," Proc. Int. Telecommun. Energy Conf., INTELEC, pp. 824–831, 2007.

[13] S. Chudjuarjeen, A. Sangswang, and C. Koompai, "An improved LLC resonant inverter for induction-heating applications with asymmetrical control," IEEE Trans. Ind. Electron., vol. 58, no. 7, pp. 2915–2925, Jul. 2011.

[14] J.-Y. Lee, Yu-Seok Jeong, and B.-M. Han, "An isolated DC/DC converter using high-frequency unregulated LLC resonant converter for fuel cell applications," IEEE Trans. Ind. Electron., vol. 58, no. 7, pp. 2926–2934, Jul. 2011.

[15] Y.C.Chuang,Y.L.Ke,H.S. Chuang, and Y..Chen,"Analysisandimplementation of half-bridge series–parallel resonant converter for battery chargers," IEEE Trans. Ind. Appl., vol. 47, no. 1, pp. 258–270, Feb. 2011

AUTHOR DETAILS

	S.Sanny Kumar, Pursuing M.tech (PS) Nalanda institute of Engineering and Technology(NIET), Siddharth Nagar, Kantepudi village, satenepalli Mandal, Guntur Dist.,A.P, India.
	N.Prasanth Babu, working as Asst.professor (EEE) at Nalanda institute of Engineering and Technology (NIET), Siddharth Nagar, Kantepudi village, satenepalli Mandal Guntur Dist.,A.P, India.